$m_b(m_Z)$ from jet production at the Z peak in the Cambridge algorithm

Mikhail Bilenky*
Institute of Physics, AS CR, 18040 Prague 8, and Nuclear Physics Institute, AS CR, 25068 Řež(Prague), Czech Republic

Susana Cabrera and Joan Fuster
IFIC, CSIC-Universitat de València, 46100 Burjassot, València, Spain

Salvador Martí
CERN, European Laboratory for Particle Physics, CH-1211 Genève, Switzerland

Germán Rodrigo
INFN - Sezione di Firenze, Largo E. Fermi 2, 50125 Firenze, Italy

Arcadi Santamaria
Departament de Física Teòrica, IFIC, CSIC-Univ. de València, 46100 Burjassot, València, Spain
(Received 1 June 1999; published 29 October 1999)

We consider the production of heavy quark jets at the Z pole at next-to-leading order (NLO) using the *Cambridge jet algorithm*. We study the effects of the quark mass in two- and three-jet observables and the uncertainty due to unknown higher-order corrections as well as due to fragmentation. We find that the three-jet observable has remarkably small NLO corrections, which are stable with respect to the change of the renormalization scale, when expressed in terms of the *running quark mass* at the m_Z scale. The size of the hadronization uncertainty for this observable remains reasonably small and is very stable with respect to changes in the jet resolution parameter y_c. [S0556-2821(99)01921-9]

PACS number(s): 13.87.Ce, 12.38.Bx, 12.38.Qk, 14.65.Fy

I. INTRODUCTION

During the last few years significant progress has been made in the understanding of the heavy quark jet production in e^+e^- annihilation both experimentally[1] and theoretically.

The DELPHI Collaboration has measured the bottom-quark mass [2,3] analyzing the e^+e^- annihilation into the three-jet final state with heavy quarks using recent next-to-leading order theoretical predictions for this process [4–10]. The DELPHI result[2] for the Durham [11] jet clustering algorithm

$$m_b(m_Z) = 2.67 \pm 0.25(\text{stat}) \pm 0.34(\text{had}) \pm 0.27(\text{theor}) \quad \text{GeV}, \tag{1}$$

was the first measurement of the b-quark mass far above the production threshold and it is the first experimental evidence (at the 2–3 σ level) of the running of a fermion mass, as predicted by the standard model. Recently, the SLAC Large Detector Collaboration has also analyzed the three- and four-jet data using the Durham and several Jade-like jet algorithms [12]. These results have been used to obtain a value for the b-quark mass [13] which is compatible with the above DELPHI result.

The heavy quark mass measurement was done under the assumption of the flavor independence of the strong interactions with the value of the strong-coupling constant α_s fixed to its world average measured in other experiments. On the other hand, assuming a given b-quark mass value obtained from low-energy measurements, and comparing the value of α_s measured from the heavy quark three-jet final state with the one measured from the production of light quarks, one can perform a test of the flavor universality of the strong interaction. Such a test was performed recently [3,12,14] and no deviation from the QCD prediction was found. The next-to-leading order QCD predictions with heavy quark mass corrections from Refs. [4–10] were used in these studies.

There are three main sources of uncertainties in the DELPHI analysis. The first one has a statistical nature. The second error is due to the uncertainty in the hadronization corrections. It was evaluated [3] using different Monte Carlo models simulating the hadronization process. The third one is due to our ignorance of higher-order perturbative corrections in the theoretical predictions at the partonic level. The last uncertainty was estimated by varying the renormalization scale in the calculations and by using different renormalization schemes, i.e., expressing intermediate results in terms of either the perturbative pole quark mass or the running quark mass.

The value of the b-quark mass measured at the Z peak (1) is found to be in good agreement with the determinations of the b-quark mass at low energy from Υ- and B-meson spectroscopy [15], when compared at the same scale. However, the uncertainties in $m_b(m_Z)$ are larger. Thus, it would be

*On leave from JINR, 141980 Dubna, Russian Federation.

[1]See [1] for a review of recent experimental results.

[2]The modified minimal subtraction scheme ($\overline{\text{MS}}$) definition for the running mass at the m_Z scale was used.

desirable to reduce this error by finding new observables which may show a better theoretical and hadronization properties.

In this paper we study quark mass effects in heavy quark jet production by using the Cambridge jet clustering algorithm [16,17]. We also study the possibility of reducing the uncertainties in the measurement of the *b*-quark mass at the *Z* pole. We consider two jet observables and estimate the errors in their theoretical predictions due to the unknown higher orders by varying the renormalization scale and considering different renormalization schemes. We discuss also the size of the uncertainty due to the hadronization process. Some preliminary results of this study were reported in [18,19].

II. THE CAMBRIDGE ALGORITHM AND THE DECAY $Z\to 3$ JETS AT THE NEXT-TO-LEADING ORDER

The Cambridge [16] jet clustering algorithm is a modified version of the popular Durham [11] algorithm that has been introduced recently in order to reduce at low y_c the formation of spurious jets with low transverse momentum particles. Consequently, compared to Durham, it allows one to explore regions of smaller y_c, while still keeping higher-order corrections relatively small. It is important to note that at low y_c the statistical experimental error for three-jet and four-jet production is expected to be smaller, and the sensitivity to the quark mass increases.

In the Durham algorithm one finds the minimal test variable y_{ij} defined as

$$y_{ij}=2\frac{\min(E_i^2,E_j^2)}{s}(1-\cos\theta_{ij}), \tag{2}$$

for all possible pair combinations of the particles and compare it with the jet-resolution parameter, y_c. In Eq. (2) E_i and E_j denote the energies of particles[3] *i* and *j*, θ_{ij} is the angle between their three momenta and *s* is the center-of-mass energy squared. If $y_{ij}<y_c$, the two particles *i* and *j* are combined into a new pseudoparticle with momentum

$$p_k=p_i+p_j. \tag{3}$$

The procedure is repeated again and again until $y_{ij}>y_c$ for all pairs of (pseudo)particles. The number of (pseudo)particles at the end defines the number of jets.

The Cambridge algorithm is defined by the same test variable, Eq. (2), and the same recombination rule, Eq. (3), as Durham. The new ingredient of the Cambridge algorithm is the so-called *ordering variable*

$$v_{ij}=2(1-\cos\theta_{ij}). \tag{4}$$

In this algorithm, first, the pair of particles, which has minimal ordering variable v_{ij}, is selected. Then one computes y_{ij} for this pair of particles, and, if $y_{ij}<y_c$, the two particles are recombined into a pseudoparticle according to Eq. (3). But if $y_{ij}>y_c$, the softer particle from this pair is assigned to a resolved jet. This last step is called ''soft freezing.''

Because of the additional step in the jet-finding iterative procedure, the Cambridge scheme turns out to be more complex and has a number of peculiar properties [20]. Let us mention only one example. In Jade-like algorithms, including Durham, one can always define a transition value of y_c, such that a multiparton event classified as a *n*-jet event becomes a $n+1$-jet event, when the value of y_c is slightly decreased. However, as pointed out in [20], this property is lost in the Cambridge algorithm, since, due to the presence of the ordering parameter, the sequence of clustering depends on the value of y_c. As a result the number of jets is not a monotonic function of y_c and it can change by a non-unit number at some transition value of y_c.

With the above definitions one can show that the cross section of the e^+e^- annihilation into three jets calculated at the leading order (LO) is the same in both Cambridge and Durham algorithms. This happens because only three-parton final-state configurations contribute at LO to the three-jet cross section. Instead, the four-jet production cross section at the LO is different in the two schemes.

At next-to-leading order (NLO) the predictions for the three-jet production cross section for the two algorithms are different. Schematically, the NLO calculation of $e^+e^-\to 3$ jets was performed as follows. In this case the three-jet cross section receives contributions not only from one-loop corrected three-parton final states, but also from four-parton processes. In the latter process two of the four partons are combined in order to produce a three-jet final state. The ultraviolet (UV) divergences encountered in the calculation of the three-parton contribution at the one-loop level were removed by the renormalization of the parameters of the QCD Lagrangian. The infrared (IR) divergences[4] remaining in this part, which are due to the presence of massless gluons in the loop, were canceled in the final result for the three-jet transition probability by adding an appropriate contribution from the four-parton final state. In the latter contribution, which is a purely tree-level one, the IR divergences appear due to the radiation of soft and/or collinear massless gluons. To separate the IR divergent part of the four-parton contribution, the phase-space slicing method (see [21], and references cited therein) has been used. In this method the integration over a thin slice at the edge of the phase space (containing the soft and the collinear singularities) is performed analytically. Then, the IR singularities coming from three- and four-parton final states are canceled analytically. The remaining finite pieces from both three-parton and four-parton processes are integrated numerically over the three-jet phase space defined by the specific jet algorithm. The four-jet cross section at the leading order, which is IR finite, is also obtained by numerical integration over the four-jet part of the four-parton phase space.

[3]By the word ''particles'' we mean here both the real hadrons detected at experiment and the partons entering the theoretical calculation.

[4]Dimensional regularization was used to regularize both ultraviolet (UV) and infrared (IR) singularities in the whole calculation.

Details of the NLO calculation for the Durham and some other popular jet clustering algorithms were presented in [4–6]. In the case of the Cambridge algorithm, although all principal calculational steps of the three-jet heavy quark production in e^+e^- annihilation at NLO remain the same as in other algorithms, the practical implementation of this scheme turned out to be more involved due to more complex realization of the Cambridge jet finder.

III. THE OBSERVABLES

In this paper we study in detail the following ratio of three-jet rates in the Cambridge jet algorithm:

$$R_3^{bl}=\frac{\Gamma_{3j}^b(y_c)/\Gamma^b}{\Gamma_{3j}^l(y_c)/\Gamma^l}. \tag{5}$$

In the above equation Γ_{3j}^b and Γ^b stand, respectively, for the three-jet and the total decay widths of the Z boson with a b quark in the final state. Analogously, the quantities with the superscript l denote the sum of the decay widths into light quarks ($l=u,d,s$) which all are considered massless.

The ratio R_3^{bl} can be written in the form of the following expansion in α_s:

$$R_3^{bl}=1+\frac{\alpha_s(\mu)}{\pi}a_0(y_c)+r_b\left(b_0(r_b,y_c)+\frac{\alpha_s(\mu)}{\pi}b_1(r_b,y_c)\right), \tag{6}$$

where $r_b=M_b^2/s$, with M_b being the heavy quark pole mass, and $s=m_Z^2$ at the Z peak.

Let us remark that the double ratio in Eq. (5) differs slightly from the one R_3^{bd}, considered in [22,4] with a normalization to the Z-decay width of only one light flavor, the d quark. In contrast to R_3^{bl}, such a double ratio is equal to the unit for a vanishing b-quark mass. The main difference between the two observables, R_3^{bl} and R_3^{bd}, is due to the triangle one-loop diagrams [23], which give a nonzero contribution even in the case of massless b quarks taken into account by a function $a_0(y_c)$ in Eq. (6). The difference is, however, very small numerically, smaller than 0.2%.

The functions b_0 and b_1 in Eq. (6) describe, accordingly, the quark mass effects at the leading and the next-to-leading order in the strong coupling and depend on the jet clustering scheme. Although, for convenience, the leading polynomial dependence on r_b has been factorized out in Eq. (6), the exact dependence on the heavy quark mass is kept in the functions $b_0(r_b,y_c)$ and $b_1(r_b,y_c)$.

Using the known relationship between the perturbative pole mass and the $\overline{\rm MS}$ scheme running mass [24],

$$M_b^2=m_b^2(\mu)\left[1+\frac{2\alpha_s(\mu)}{\pi}\left(\frac{4}{3}-\log\frac{m_b^2}{\mu^2}\right)\right], \tag{7}$$

we can re-express Eq. (6) in terms of the running mass $m_b(\mu)$. Then, keeping only terms of order $\mathcal{O}(\alpha_s)$ we obtain

$$R_3^{bl}=1+\frac{\alpha_s(\mu)}{\pi}a_0(y_c)+\overline{r}_b(\mu)\times\left(b_0(\overline{r}_b,y_c)+\frac{\alpha_s(\mu)}{\pi}\overline{b}_1(\overline{r}_b,y_c,\mu)\right), \tag{8}$$

where $\overline{r}_b(\mu)=m_b^2(\mu)/m_Z^2$ and the new function $\overline{b}_1$ is related to b_0 and b_1, introduced in Eq. (6), via

$$\overline{b}_1(\overline{r}_b,y_c,\mu)=b_1(\overline{r}_b,y_c)+2b_0(\overline{r}_b,y_c)\times\left(\frac{4}{3}-\log\overline{r}_b+\log\frac{\mu^2}{m_Z^2}\right). \tag{9}$$

Effectively, the use of $m_b(\mu)$, instead of M_b, corresponds to the use of a different renormalization scheme. Although at the perturbative level both expressions, Eqs. (6) and (8), are equivalent, numerically they give different answers since different higher-order contributions are neglected. The spread of the results gives an estimate of the size of higher-order corrections.

As discussed in the previous section, the phase-space integration (up to fivefold) in the calculation of the NLO decay width of the Z boson into three jets is done numerically. This numerical integration is rather time consuming. Hence, we found it very convenient to fit the numerical results with relatively simple analytical functions. Because very small y_c values are considered in the case of the Cambridge scheme, these fits are more complex and involve more parameters than the ones for the Durham algorithm described in [4]. A Fortran code containing the fits to the functions b_0 and b_1 (or $\overline{b}_1$)[5] can be obtained from the authors upon request. The numerical results for R_3^{bl} are presented in the next section.

In the next section we also give numerical results for the ratio of differential two-jet rates, defined as follows:

$$D_2^{bl}=\frac{[\Gamma_{2j}^b(y_c+\Delta y_c/2)-\Gamma_{2j}^b(y_c-\Delta y_c/2)]/\Gamma^b}{[\Gamma_{2j}^l(y_c+\Delta y_c/2)-\Gamma_{2j}^l(y_c-\Delta y_c/2)]/\Gamma^l}. \tag{10}$$

Here, Γ_{2j}^b and Γ_{2j}^l denote the two-jet decay widths of the Z boson with a b quark and light quarks in the final state, correspondingly. The two-jet decay width at the order $\mathcal{O}(\alpha_s^2)$ is calculated from the three- and the four-jet widths through the identity

$$\Gamma^q=\Gamma_{2j}^q+\Gamma_{3j}^q+\Gamma_{4j}^q,$$

where q is the quark flavor and Γ_{4j}^q is the four-jet decay width at the leading order. The value of Δy_c in Eq. (10) should be chosen small enough. We fix $\Delta y_c=0.001$ in the numerical analysis.

The differential ratio D_2^{bl} is interesting because it contains different information than the ratio R_3^{bl}. In addition, while

[5]Although, the two functions b_1 and $\overline{b}_1$ are related via Eq. (9) we performed independent fits for these functions.

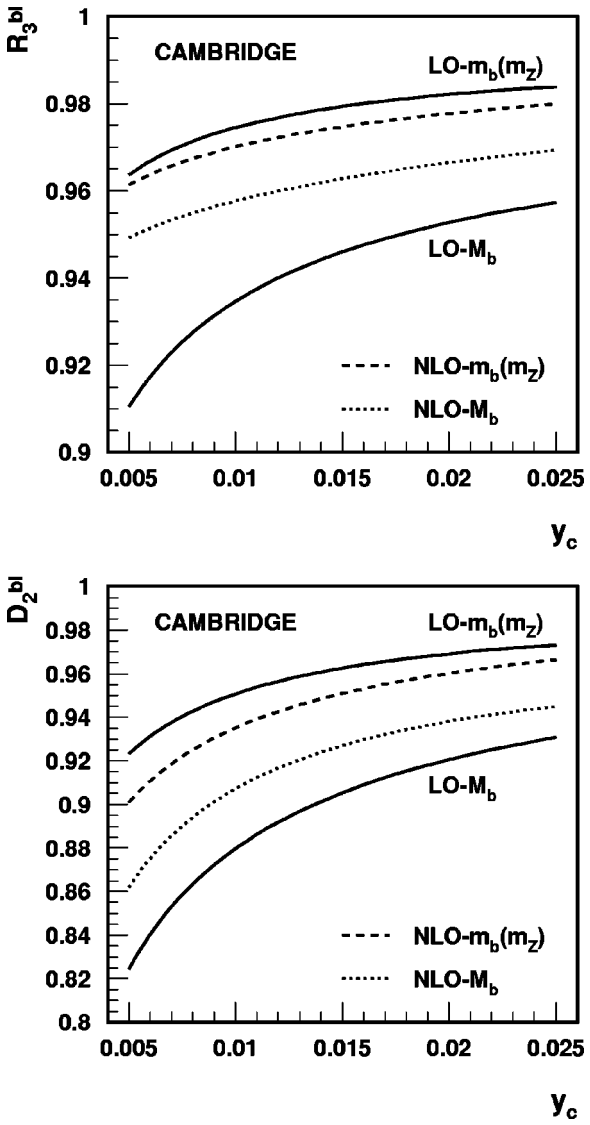

FIG. 1. The observables R_3^{bl} and D_2^{bl} as a function of y_c in the Cambridge algorithm at the NLO. The dotted lines give the NLO corrected values using Eq. (6) for a pole mass of $M_b=4.6$ GeV. The dashed lines give the observables at the NLO using Eq. (8) for a running mass of $m_b(m_Z)=2.8$ GeV. The renormalization scale is fixed to $\mu=m_Z$ and $\alpha_s(m_Z)=0.118$. For comparison we also plot the LO results for $M_b=4.6$ GeV (lower solid lines) and $m_b(m_Z)=2.8$ GeV (upper solid lines).

values of R_3^{bl} measured at different y_c are strongly correlated, the differential rate D_2^{bl} can be analyzed as a function of y_c. The whole consideration of R_3^{bl} discussed above is also applied here. For D_2^{bl} we use expansions in α_s similar to those in Eqs. (6) and (8), see [5], and we fit the corresponding LO and NLO numerical results to simple analytical functions equivalent to b_0 and b_1 $(\overline{b_1})$.

IV. PERTURBATIVE RESULTS

In Fig. 1 we present the results for the two observables studied, R_3^{bl} and D_2^{bl}, as functions of the jet-resolution parameter y_c in the Cambridge algorithm. We plot the NLO results written either in terms of the pole mass [Eq. (6)] with $M_b=4.6$ GeV, or in terms of the running quark mass at m_Z [Eq. (8)] with $m_b(m_Z)=2.8$ GeV. The renormalization scale is fixed to $\mu=m_Z$ and $\alpha_s(m_Z)=0.118$. For comparison we also show R_3^{bl} and D_2^{bl} at LO when the value of the pole mass, M_b, or the running mass at m_Z, $m_b(m_Z)$, is used for the quark mass. Note that one cannot distinguish between different definitions of the quark mass in the lower order calculation. Mass effects monotonically grow for decreasing y_c, they are very significant for both observables and in the case of D_2^{bl} exceed 10% for small values of y_c.

From this figure one sees a remarkable feature of the NLO result in the considered range of y_c, $0.005<y_c<0.025$, for the Cambridge scheme: the NLO corrections, in the case when the running mass is used are significantly smaller, especially for R_3^{bl}, than the corrections in the case with the parametrization in terms of the pole mass. In other words, using the running mass at the m_Z scale in the LO calculations takes into account the bulk of the NLO corrections. This situation, although does not guarantee, however, suggests that also next-to-next-to-leading and higher-order corrections are small for the observables parametrized in terms of the running mass at the m_Z scale, i.e., one has a better description of mass effects in terms of a short distance parameter, $m_b(m_Z)$, than in terms of a low-energy parameter like the perturbative pole mass.

The theoretical prediction for the observables studied contains a residual dependence on the renormalization scale μ: when written in terms of the pole mass it only comes from the μ dependence in $\alpha_s(\mu)$, when written in terms of the running mass it comes from both $\alpha_s(\mu)$ and the incomplete cancellation of the μ dependences between $m_b(\mu)$ and the logs of μ which appear in Eq. (9). The dependence on μ is usually regarded as an estimate of the effect of the unknown higher-order perturbative corrections. In Fig. 2(a) we present the μ dependence of the two NLO predictions, the pole mass prediction (NLO-M_b) given by Eq. (6) and the running mass prediction [NLO-$m_b(m_Z)$] given by Eq. (8), for the ratio R_3^{bl} in the range $m_Z/10<\mu<m_Z$ at a fixed value of y_c. We use the following one-loop evolution equations:

$$a(\mu)=\frac{a(m_Z)}{K}, \quad m_b(\mu)=m_b(m_Z)K^{-\gamma_0/\beta_0}, \qquad (11)$$

where $a(\mu)=\alpha_s(\mu)/\pi$, $K=1+a(m_Z)\beta_0\log(\mu^2/m_Z^2)$ and

$$\beta_0=\frac{1}{4}\left[11-\frac{2}{3}N_F\right], \quad \gamma_0=1,$$

with $N_F=5$ the number of active flavors, to obtain $\alpha_s(\mu)$ and $m_b(\mu)$ from $\alpha_s(m_Z)=0.118$ and $m_b(m_Z)=2.8$ GeV. The NLO-$m_b(m_Z)$ result (dashed line) shows a remarkable stability with respect to the variation of the renormalization scale and the corrections with respect to the LO prediction [LO-$m_b(m_Z)$] remain small for all the values of μ. Instead, the NLO-M_b prediction (dotted line) has noticeably stronger dependence on the renormalization scale. The NLO corrections in this case remain sizable for all the values of μ and

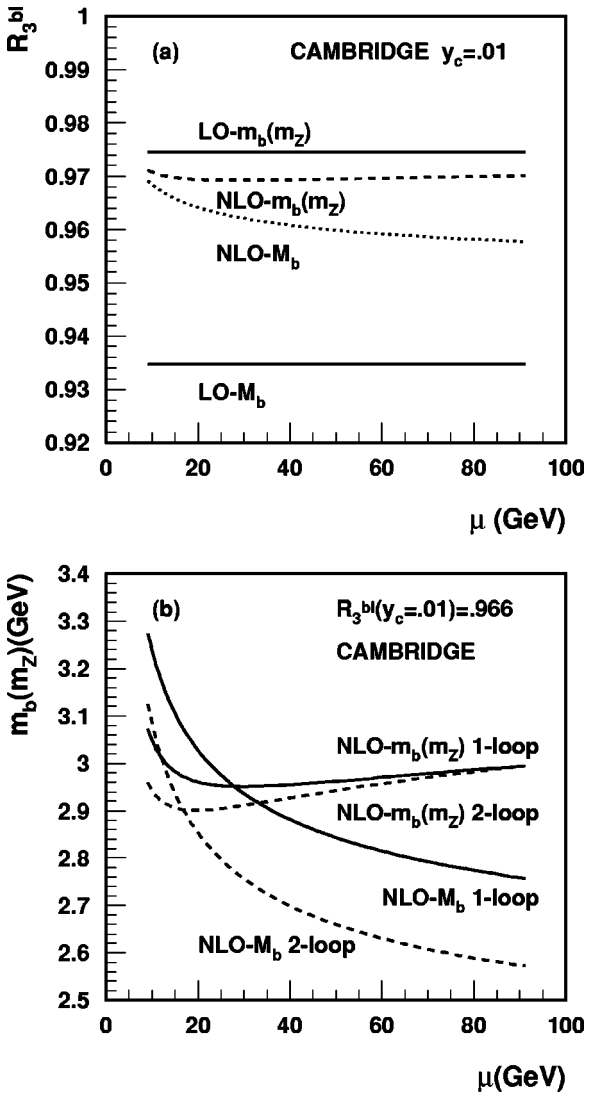

FIG. 2. (a) Renormalization scale dependence for a fixed value of y_c. Same labels as in Fig. 1. (b) Extracted value of $m_b(m_Z)$ from a fixed value of R_3^{bl} using either the pole mass expression (NLO-M_b) in Eq. (6) or the running mass expression [NLO-$m_b(m_Z)$] in Eq. (8) as explained in the text. Solid lines obtained by using one-loop running evolution equations to connect the results at different scales and dashed lines obtained by using two-loop expressions.

increase for decreasing μ. Note also that, as one would expect, for low values of μ the two NLO predictions, in terms of the running mass and in terms of the pole mass, become very close to each other.

For a given value of R_3^{bl} we can solve Eq. (6) [or Eq. (8)] with respect to the quark mass. The result, shown in Fig. 2(b) for a fixed value of R_3^{bl}, depends on which equation was used and has a residual dependence on the renormalization scale μ. The curves in Fig. 2(b) are obtained in the following way: first from Eq. (8) we directly obtain for an arbitrary value of μ between m_Z and $m_Z/10$ a value for the bottom-quark running mass at that scale, $m_b(\mu)$, and then using Eq. (11) we get a value for it at the Z scale, $m_b(m_Z)$. Second, using Eq. (6) we extract, also for an arbitrary value of μ between m_Z and $m_Z/10$, a value for the pole mass, M_b. Then we use Eq. (7) at $\mu=M_b$ and again Eq. (11) to perform the evolution from $\mu=M_b$ to $\mu=m_Z$ and finally get a value for $m_b(m_Z)$. The two procedures, denoted as NLO-$m_b(m_Z)$ and NLO-M_b, respectively, give a different answer since different higher orders have been neglected in the intermediate steps. The maximum spread of the two results in the whole μ-range under consideration can be interpreted as an estimate of the size of higher-order corrections, i.e., of the theoretical error in the determination of the bottom-quark mass from the experimental measurement of R_3^{bl}.

We see from Fig. 2(b) that the first approach is very stable with respect to the choice of the scale used in Eq. (8). The obtained b-quark mass, $m_b(m_Z)$, varies only ± 50 MeV when the scale is varied in the range $\mu=m_Z$ and $\mu=m_Z/10$. In the same range of μ, the estimated error in the Durham algorithm was found [4] to be ± 200 MeV. On the contrary, if one uses Eq. (6) the extracted quark mass has a strong scale dependence, especially for small μ values and the estimated error is very sensitive to the choice of the smallest possible value of the renormalization scale. Cutting as before at $\mu=m_Z/10$, the extracted pole mass varies in the range ± 300 MeV which is translated into ± 240 MeV for $m_b(m_Z)$. Let us note that a further ± 20 MeV should be added due to the uncertainty in the strong-coupling constant $\Delta\alpha_s(m_Z)=\pm 0.003$.

Although, our observables are formally of order $\mathcal{O}(\alpha_s)$ and, therefore, compatible with the use of one-loop renormalization-group equations (RGE's) to connect the running parameters at different scales, as a check of the stability of our results we have also repeated the analysis using two-loop evolution equations [25]

$$a(\mu)=\frac{a(m_Z)}{K+a(m_Z)b_1\left(L+a(m_Z)b_1\dfrac{1-K+L}{K}\right)},$$

$$m_b(m_Z)=m_b(\mu)K^{g_0}\frac{1+a(m_Z)c_1}{1+a(\mu)c_1}, \tag{12}$$

where $L=\log K$ and $c_1=g_1-b_1g_0$ with $b_1=\beta_1/\beta_0$, $g_i=\gamma_i/\beta_0$ and

$$\beta_1=\frac{1}{16}\left[102-\frac{38}{3}N_F\right], \quad \gamma_1=\frac{1}{16}\left[\frac{202}{3}-\frac{20}{9}N_F\right]. \tag{13}$$

The use of two-loop RGE's corresponds to the dashed lines in Fig 2(b). Again a value of the quark mass extracted via the running mass parametrization remains more stable with respect to variation of the scale μ and changes only slightly. The mass extracted through the pole mass receives a significant shift of 200 MeV when the two-loop RGE'S are used.

V. HADRONIZATION CORRECTIONS

In the DELPHI analysis on the measurement of the b-quark mass effects based on the Durham jet clustering algorithm the impact of the fragmentation process on the observable R_3^{bl} was studied [3] and quantified by adding in quadrature two different source of errors. The first uncer-

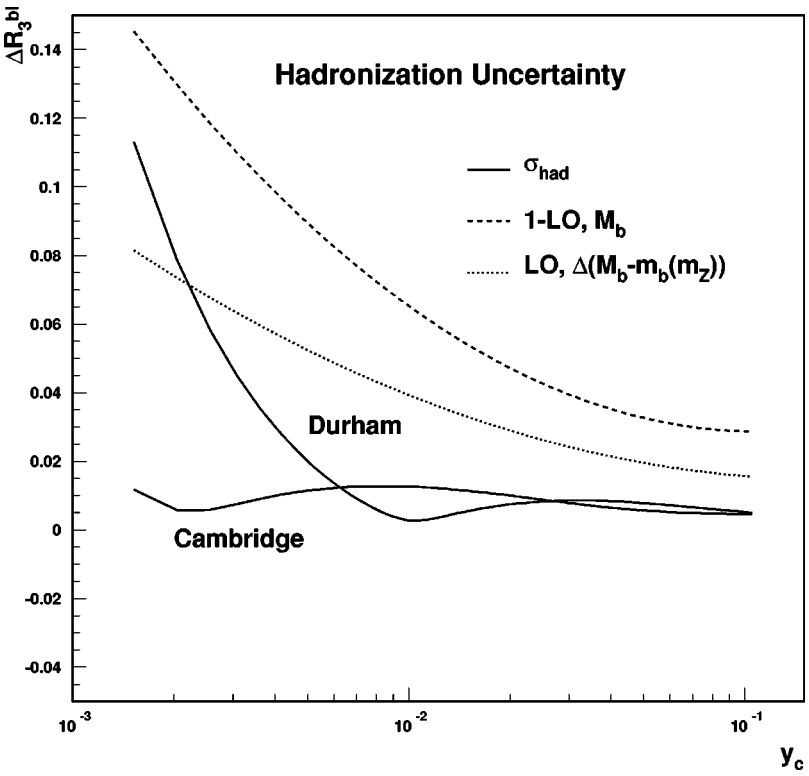

FIG. 3. Comparison of the hadronization uncertainty ($\sigma_{\rm had}$) obtained when using either the Cambridge or Durham algorithm. The dashed curve shows the mass correction at LO for the pole mass, $M_b=4.6$ GeV. The dotted curve indicates the value of the difference between the LO predictions for the two mass values, $M_b=4.6$ GeV and $m_b(m_Z)=2.8$ GeV. The Cambridge algorithm is observed to have a larger stable region on y_c than Durham reaching at the same time a higher sensitivity to both the mass correction and the difference between the two LO predictions.

tainty $\sigma_{\rm tun}$ was obtained by varying the most relevant parameters of the string fragmentation model incorporated in JETSET [26] within an interval of $\pm 2\sigma$ from its central value as tuned by DELPHI [27] and explained in Ref. [3]. The second uncertainty $\sigma_{\rm mod}$ was the result of analyzing the dependence on the fragmentation model itself by comparing the HERWIG [28] model with JETSET [26]. The difference on the fragmentation correction factors obtained for each model were considered as a source of systematic errors. This in fact was the largest contribution to the total error of the measurement. The final correction adopted was the average of those two models and the *fragmentation model* uncertainty ($\sigma_{\rm mod}$) was taken to be half of their difference. The total error due to the lack of knowledge on the hadronization process was expressed as

$$\sigma_{\rm had}(y_c)=\sqrt{\sigma^2_{\rm tun}(y_c)+\sigma^2_{\rm mod}(y_c)} \tag{14}$$

which at $y_c=0.02$ in the Durham scheme was $\sigma_{\rm had}(y_c)=0.007$ [3] and its dependence as a function of y_c is shown in Fig. 3. The decision of the measurable y_c interval region, $y_c>0.015$ was also connected to the fragmentation correction which was required to be relatively flat and the four-jet contribution small ($\leqslant 2\%$). For comparison purposes, an equivalent analysis has been performed using the new Cambridge jet reconstruction algorithm and the results obtained are also presented in Fig. 3. A larger flat y_c region is observed in the case of Cambridge with respect to Durham which can be extended up to $y_c=0.004$ with the four jet contribution still being small, $\leqslant 8\%$. The total absolute error is higher for Cambridge than for Durham but the relative sensitivity to the mass correction is higher for Cambridge at y_c values around 0.005 than for Durham at y_c values around 0.02. In Fig. 3 the difference between the theoretical prediction of R_3^{bl} at LO in terms of the pole mass, $M_b=4.6$ GeV with respect to that obtained using the running mass $m_b(m_Z)=2.8$ GeV is also shown. A higher sensitivity to this difference is again found for the new Cambridge jet algorithm in the valid, flat, y_c region ($y_c>0.004$) thus enabling a more significant test on which of both predictions agrees better with data.

VI. CONCLUSIONS

We have calculated the next-to-leading order QCD corrections to the heavy quark three-jet production cross section in e^+e^- annihilation as well as the leading-order four-jet production cross section using the new Cambridge jet clustering algorithm. The hadronization corrections were also estimated. Comparing with previous studies, this algorithm allows one to extend the analysis into a region of smaller values of the jet resolution parameter, down to $y_c\approx 0.004$, where the sensitivity to the heavy quark mass effects increase.

In particular, we have studied in detail the double ratio R_3^{bl} and the differential double ratio D_2^{bl}. We have compared the NLO results expressed in terms of the perturbative pole mass and in terms of the running mass of the heavy quark at the m_Z scale. We found that the NLO corrections in the case when the running mass was used are remarkably small. This is especially true for R_3^{bl}, where tree-level expressions in terms of $m_b(m_Z)$ give a very good approximation to the complete NLO result, which, when expressed in terms of $m_b(m_Z)$, is almost independent of the renormalization scale.

In contrast, the calculations done in terms of the pole quark mass have sizable NLO corrections with a strong renormalization scale dependence. The hadronization corrections also favor the use of the Cambridge algorithm with respect to Durham by keeping a relatively stable uncertainty for small y_c. Summarizing, the results of this paper indicate that a new determination of the *b*-quark mass with the Cambridge jet algorithm will improve our present understanding on quark mass effects at the Z peak.

ACKNOWLEDGMENTS

This work has been supported by the CICYT under Grant No. AEN-96-1718, by DGESIC under Grant No. PB97-1261 and by the Generalitat Valenciana under Grant No. GV98-01-80. The work of G.R. has also been supported by INFN and E.U. QCDNET Contract No. FMRX-CT98-0194. The work of M.B. was partly supported by Grant No. GAČR-2020506.

[1] SLD Collaboration, P.N. Burrows *et al.*, hep-ex/9808017.
[2] S. Martí Garcia, J. Fuster, and S. Cabrera, Nucl. Phys. B (Proc. Suppl.) **64**, 376 (1998).
[3] DELPHI Collaboration, P. Abreu *et al.*, Phys. Lett. B **418**, 430 (1998).
[4] G. Rodrigo, A. Santamaria, and M. Bilenky, Phys. Rev. Lett. **79**, 193 (1997).
[5] G. Rodrigo, M. Bilenky, and A. Santamaria, Nucl. Phys. **B554**, 257 (1999); G. Rodrigo, A. Santamaria, and M. Bilenky, J. Phys. G **25**, 1593 (1999).
[6] G. Rodrigo, Nucl. Phys. B (Proc. Suppl.) **54A**, 60 (1997).
[7] A. Brandenburg and P. Uwer, Nucl. Phys. **B515**, 279 (1998).
[8] W. Bernreuther, A. Brandenburg, and P. Uwer, Phys. Rev. Lett. **79**, 189 (1997).
[9] C. Oleari, ''Next-to-leading order corrections to the production of heavy flavor jets in e^+e^- collisions,'' hep-ph/9802431.
[10] P. Nason and C. Oleari, Nucl. Phys. **B521**, 237 (1998); Phys. Lett. B **407**, 57 (1997).
[11] S. Catani, Y.L. Dokshitser, M. Olsson, G. Turnock, and B.R. Webber, Phys. Lett. B **269**, 432 (1991).
[12] SLD Collaboration, K. Abe *et al.*, Phys. Rev. D **59**, 012002 (1999).
[13] A. Brandenburg *et al.*, ''Measurement of the running b-quark mass using $e^+e^-\to b\bar{b}g$ events,'' hep-ph/9905495.
[14] OPAL Collaboration, G. Abbiendi *et al.*, hep-ex/9904013.
[15] M. Jamin and A. Pich, Nucl. Phys. **B507**, 334 (1997); V. Giménez, G. Martinelli, and C.T. Sachrajda, Nucl. Phys. B (Proc. Suppl.) **53**, 365 (1997); Phys. Lett. B **393**, 124 (1997).
[16] Y.L. Dokshitser, G.D. Leder, S. Moretti, and B.R. Webber, J. High Energy Phys. **08**, 001 (1997).
[17] S. Moretti, L. Lonnblad, and T. Sjöstrand, J. High Energy Phys. **08**, 001 (1998).
[18] G. Rodrigo, A. Santamaria, and M. Bilenky, hep-ph/9812433; M. Bilenky, G. Rodrigo, and A. Santamaria, hep-ph/9811465.
[19] DELPHI Collaboration, J. Fuster, S. Cabrera, and S. Martí, contributing paper No. 152 to ICHEP98 Conference, Vancouver, 1998.
[20] S. Bentvelsen and I. Meyer, Eur. Phys. J. C **4**, 623 (1998).
[21] S. Keller and E. Laenen, Phys. Rev. D **59**, 114004 (1999).
[22] M. Bilenky, G. Rodrigo, and A. Santamaria, Nucl. Phys. **B439**, 505 (1995).
[23] K. Hagiwara, T. Kuruma, and Y. Yamada, Nucl. Phys. **B358**, 80 (1991).
[24] R. Tarrach, Nucl. Phys. **B183**, 384 (1981).
[25] G. Rodrigo, A. Pich, and A. Santamaria, Phys. Lett. B **424**, 367 (1998).
[26] T. Sjöstrand, Comput. Phys. Commun. **39**, 346 (1986).
[27] DELPHI Collaboration, P. Abreu *et al.*, Z. Phys. C **73**, 11 (1996).
[28] G. Marchesini *et al.*, Comput. Phys. Commun. **67**, 465 (1992).